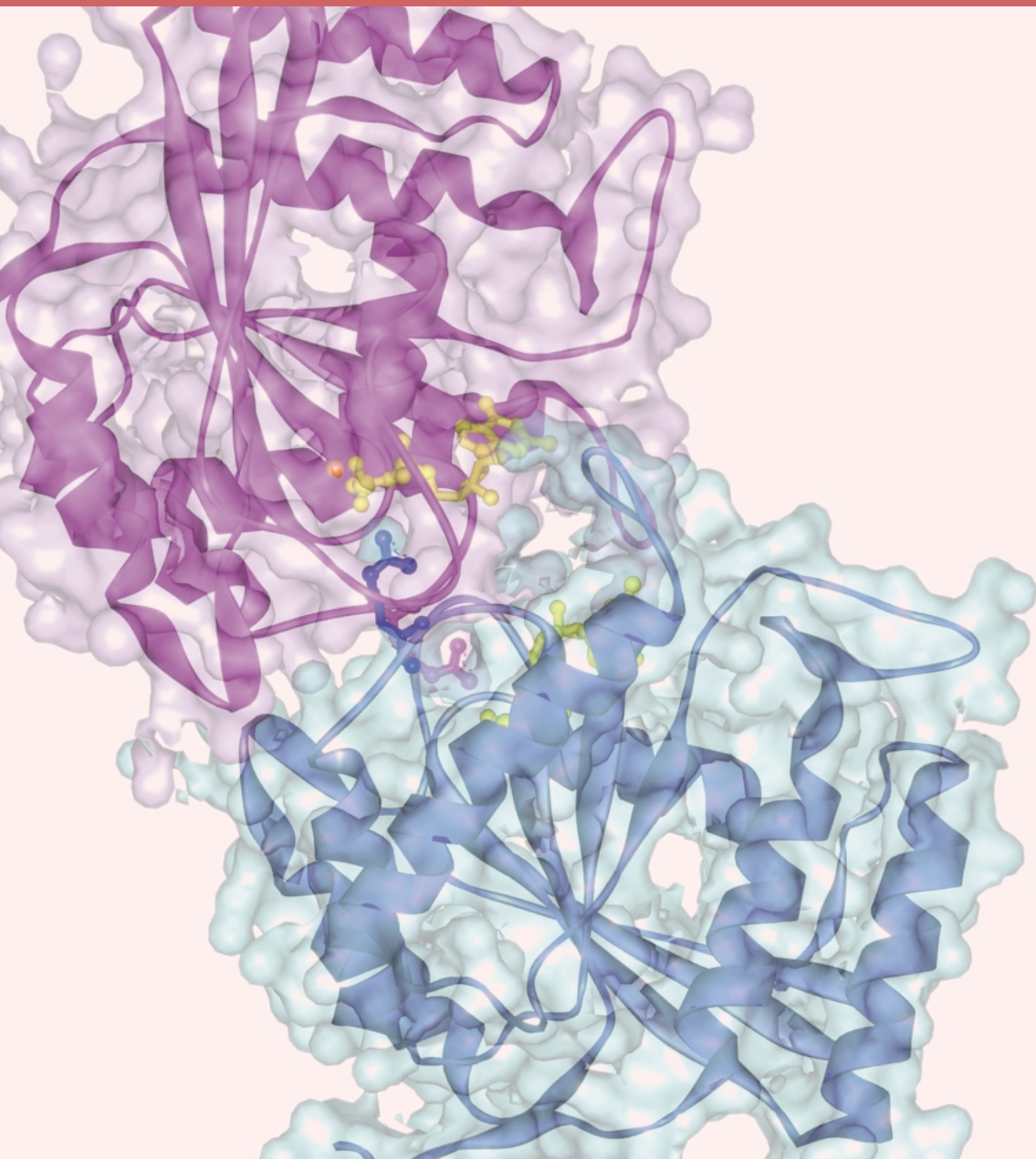


Highlights



5-1 "Devil's Flower" Blooming in NaV_2O_5

The most exciting phase diagram in statistical physics - **Devil's Flower** [1] - has been reproduced experimentally in the Temperature-Pressure (T - P) phase diagram of NaV_2O_5 [2].

In 1985, Bak *et al.* proposed a simple model, which is well known as the ANNNI (Axial Next Nearest Neighbor Ising) model at present. On the basis of such a model, they carried out theoretical calculations considering two competitive inter-layer interactions between Ising spins (see Fig.1 inset), i.e., the nearest neighbor interaction $J_1 > 0$ (ferro) and the next nearest neighbor interaction $J_2 < 0$ (antiferro) and obtained an interesting κ - T ($\kappa = -J_2/J_1$) phase diagram (see Fig. 1) in which an infinite number of commensurate phase appears as a function of κ and T . Such a phase diagram is named "**Devil's Flower**", because it seems as if an infinite number of petals bloom from the $\kappa = 0.5$ position.

A quarter-filled spin-ladder system NaV_2O_5 undergoes a novel cooperative phase transition associated at $T_c = 34$ K with its charge ordering, lattice dimerization ($2a \times 2b \times 4c$ superstructure) and spin-gap formation. By the complementary use of synchrotron X-ray structural analysis and resonant X-ray scattering (RXS) techniques at the Photon Factory, the $2a \times 2b \times 4c$ superstructure below T_c was solved unambiguously [3,4]. An oblique charge stripe pattern formed in each V_2O_5 -layer (ab -plane) is shown in Fig. 2 as A and A'. Atomic

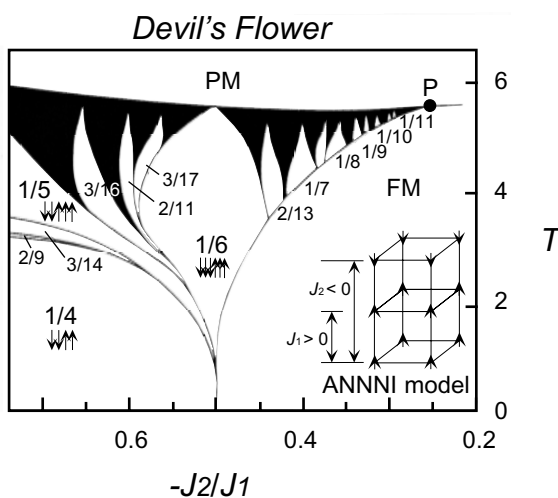


Figure 1
"Devil's Flower" (κ - T phase diagram) obtained from ANNNI model. Fractions seen in the phase diagram show the modulation wave numbers. Black regions are composed of more complicated commensurate and incommensurate phases.

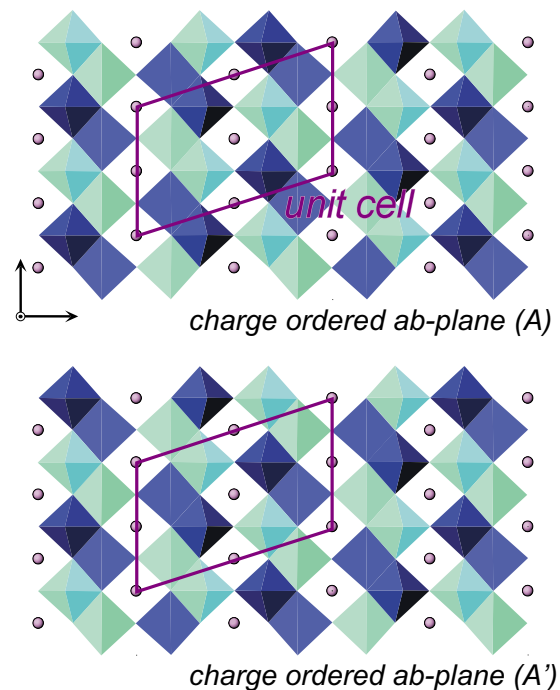


Figure 2
Schematic charge order patterns determined in ab -plane, consisting of two kinds of patterns A and A'.

shifts coupled with such a charge ordering are not shown in this figure. The charge ordering patterns called A and A' are related by a phase shift π along the b -axis, where a dark blue colored pyramid represents V^{4+}O_5 and a light blue V^{5+}O_5 . The stacking sequence of the patterns A and A' along the c -axis was unambiguously determined by the RXS as AAA'A' [4].

By application of high pressure, the stacking sequence along the c -axis drastically changes. For an overall study, we applied an oscillation photographic method (BL-1B), and for a detailed study, we used a counter method (BL-4C). Figure 3(a) presents the temperature dependence of the $[15/2, 1/2, q_c]$ superlattice Bragg position at 0.88 GPa taken at BL-1B. One can clearly see that the modulation wave number q_c changes as a function of temperature. Figure 3(b) displays the temperature dependence of *high-resolution* diffraction profiles observed along the $[13/2, 3/2, q_c]$ direction at 0.92 GPa taken at BL-4C. In this figure, a few more reflections are newly observed. It is also shown that a series of superlattice reflections with $q_c = 1/4, 1/5, 1/6$ and $3/17$ systematically appear and disappear as a function of temperature. What we observe is peak intensities coming from the atomic shifts coupled with the charge modulations [5]. This q_c sequence means that the stacking sequence along the c -axis drastically changes

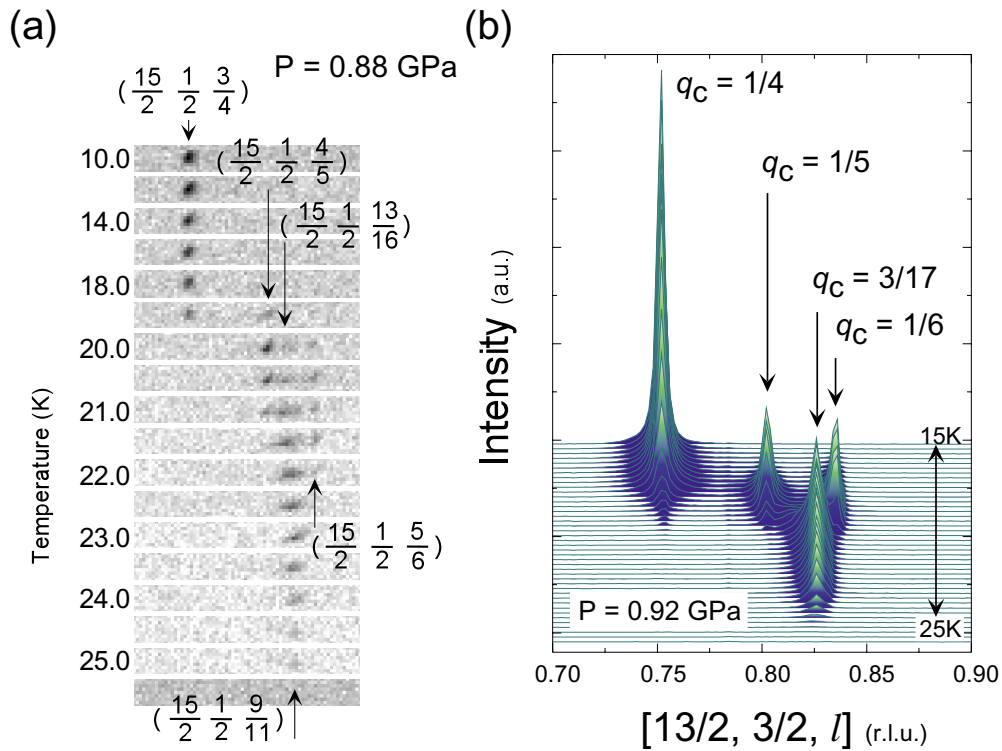


Figure 3 (a) Temperature dependence of a position of superlattice reflections $(15/2, 1/2 l)$ recorded on IP oscillation photographs at 0.88 GPa. (b) Temperature dependence of high-resolution X-ray diffraction profiles observed along the $[13/2, 3/2, q_c]$ direction at 0.92 GPa.

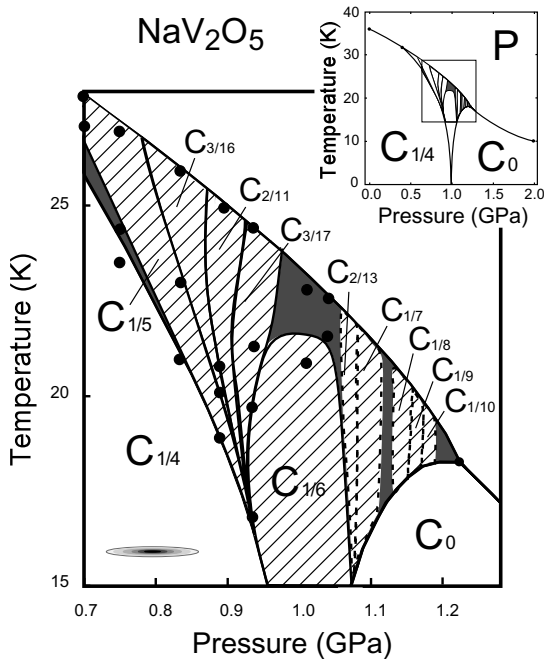


Figure 4 Experimentally obtained T - P phase diagram "Devil's Flower" of NaV_2O_5 . The hatched area shows commensurate phases unambiguously identified while the shaded area indicates more complicated higher-order commensurate or incommensurate phases.

as AAA'A'A' for $1/5$, AAAA'A'A' for $1/6$, AAA'A'A'AAAA'A' A'AAAA'A'A' for $3/17$ and so on. We also could observe the other types of q_c sequences in a wide temperature and pressure range and finally confirmed that the "Devil's Flower" is perfectly reproduced in NaV_2O_5 [2] under high pressure and low temperature (Fig. 4). A microscopic mechanism of the competitive inter-layer interaction resulting in such a phase diagram is a keen subject of further study.

K. Ohwada¹, Y. Katsuki², Y. Fujii³, M. Isobe³, Y. Ueda³, H. Nakao⁴, Y. Murakami⁴, E. Ninomiya⁵ and H. Sawa⁶ (¹JAERI/Spring-8, ²Accenture Co. Ltd., ³ISSP/Univ. of Tokyo, ⁴Tohoku Univ., ⁵Chiba Univ., ⁶KEK-PF)

References

- [1] P. Bak and J. von Boehm, *Phys. Rev. B* **21** (1980) 5297.
- [2] K. Ohwada, Y. Fujii, N. Takesue, M. Isobe, Y. Ueda, H. Nakao, Y. Wakabayashi, Y. Murakami, K. Ito, Y. Amemiya, H. Fujihisa, K. Aoki, T. Shobu, Y. Noda and N. Ikeda, *Phys. Rev. Lett.* **87** (2001) 086402.
- [3] H. Sawa, E. Ninomiya, T. Ohama, H. Nakao, K. Ohwada, Y. Murakami, Y. Fujii, Y. Noda, M. Isobe and Y. Ueda, *J. Phys. Soc. Jpn.* **71** (2001) 385; H. Sawa, *Photon Factory Activity Report 2000 #18* (2001) A 25.
- [4] Y. Katsuki, *Master Thesis (Graduate School of Science, The University of Tokyo, Mar. 2002)*; Y. Fujii *et al.* in preparation.
- [5] K. Ohwada *et al.* private communication.

5-2 Confined Water Inside Carbon Nanotubes

Single-walled carbon nanotubes (SWNTs) crystallize into bundles with a closest-packed triangular lattice, where nanometer channels are present inside and outside each SWNT. These channels can accommodate a large variety of molecules and atoms, and are expected to show exotic properties which could not occur in bulk materials. Among many materials for filling SWNTs, water would be particularly interesting because it can be found in many relevant situations in nature [1]. Recent computer simulations have demonstrated interesting properties of water in a SWNT, such as novel water conduction [2] and formation of polygonal ice tubes [3]. However, relevant experimental observation even for the adsorption of water into SWNTs has not yet been reported, except for preliminary results for water in air [4]. Thus, we performed detailed systematic X-ray diffraction (XRD) experiments for the water-SWNT system. We

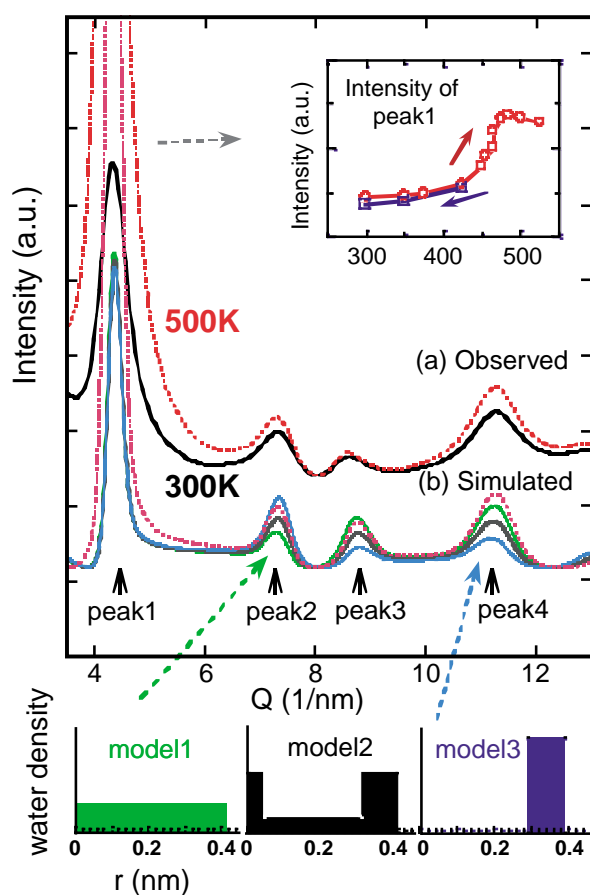


Figure 5
X-ray diffraction (XRD) profiles of water-exposed SWNT bundles. (a) Observed profiles. (b) Simulated XRD profiles for empty SWNT bundles (dotted line), water-encapsulated SWNT bundles for model 1 (green line), model 2 (black line) and model 3 (blue line). (c) Radial density distribution of water for model 1, 2 and 3. The inset is the temperature dependence of the peak 1 intensity appeared around $Q=4.3 \text{ nm}^{-1}$.

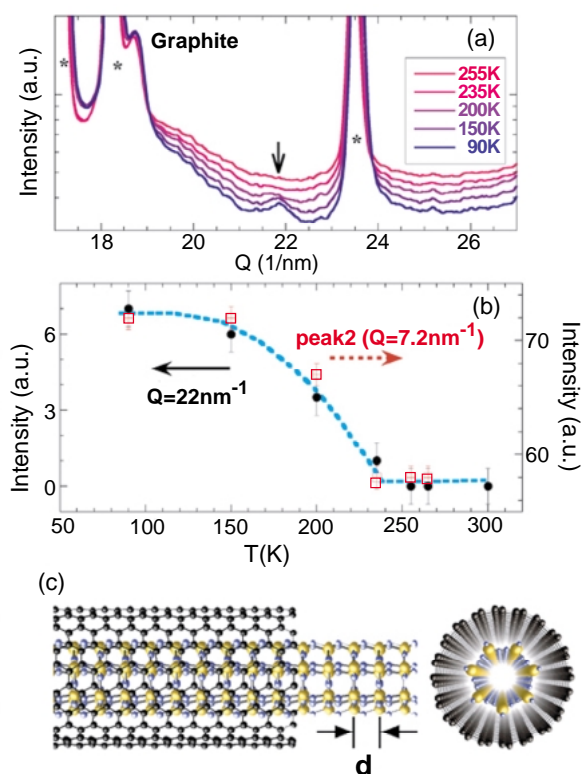


Figure 6
(a) Temperature dependence of XRD profiles in water-exposed SWNT bundles. Stars (*) are peaks due to the bulk ice. (b) Temperature dependence of the peak intensity around $Q=22 \text{ nm}^{-1}$ shown by the arrow in Fig. 2a, along with that of peak 2 around $Q=7.2 \text{ nm}^{-1}$. The background intensity due to a quartz capillary has been subtracted. (c) The proposed structure of ice-nanotube inside a SWNT. The estimated d -spacing is 0.287 nm at 90 K .

confirmed that a substantial amount of water is adsorbed inside SWNTs, but not for the interstitial channels outside SWNTs. In addition, it is found that liquid-like water at room temperature (RT) is transformed into ice-nanotubes below 235 K .

The SWNTs were sealed in a quartz capillary with water vapor at RT. Powder XRD measurements were performed using synchrotron radiation of a wavelength 0.1000 nm at BL-1B. Figure 5a shows examples of the XRD patterns taken at 300 K and 500 K . The weak intensity of peak 1 at 300 K , shown by an arrow in the figure, compared with that of pristine SWNTs (not shown here), indicated that water molecules were encapsulated inside SWNTs. But with increasing temperature, the peak 1 intensity substantially increased and approached that of pristine SWNTs above 475 K , implying that desorption of water occurred.

For further discussions, we have simulated the XRD pattern using three models for the radial density distribution of water inside the SWNT, as shown in Fig. 5(b). Irrespective of the density profile (models 1, 2 and 3), the simulation indicated that peak 1 substantially diminishes upon water adsorption inside SWNTs, as experimentally observed. Further detailed comparisons led us to conclude that the most probable density profile is given by model 2 at 300 K . With decreasing

temperature, it was found to be transformed into a tube-like distribution described by model 3 below 235 K. In addition, a new peak ascribed to the one-dimensional ordered arrangement of water molecules developed at the corresponding temperatures, as shown by an arrow in Fig. 6(a), (b). These results strongly suggest formation of the ice-nanotube inside SWNTs, as illustrated in Fig. 6(c).

**Y. Maniwa^{1,2}, H. Kataura¹, M. Abe¹, S. Suzuki¹,
Y. Achiba¹, H. Kira¹ and K. Matsuda¹ (¹Tokyo Metro.**

Univ., ²CREST)

References

- [1] M.S.P. Sanson and P.C. Biggin, *Nature* **414** (2001) 156.
- [2] G. Hummer, J.C. Rasaiah and J.P. Noworyta, *Nature* **414** (2001) 188.
- [3] K. Koga, G.T. Gao, H. Tanaka and X.C. Zeng, *Nature* **412** (2001) 802.
- [4] Y. Maniwa, Y. Kumazawa, Y. Saito, H. Tou, H. Kataura, H. Ishii, S. Suzuki, Y. Achiba, A. Fujiwara and H. Suematsu, *Jpn. J. Appl. Phys.* **38** (1999) L668.